NANOSYSTEMS:
PHYSICS, CHEMISTRY, MATHEMATICS

Original article

Kapuganti V. Divya Lakshmi, et al. *Nanosystems: Phys. Chem. Math.*, 2022, **13** (4), 438–444.
http://nanojournal.ifmo.ru
DOI 10.17586/2220-8054-2022-13-4-438-444

Enhancement of photocatalytic and antibacterial activity performance of Mn–S co-doped TiO_2 nanocatalyst under visible light

Kapuganti V. Divya Lakshmi[1,2], Tirukkovalluri Siva Rao[2], Gorli Divya[2]

[1]Sri Satya Sai University for Human Excellence, Kalaburagi, Karnataka, India

[2]Department of Inorganic and Analytical Chemistry, Andhra University, Visakhapatnam 530003, India

Corresponding author: Tirukkovalluri Siva Rao, sivaraotvalluri.16@gmail.com

ABSTRACT This paper aims to explore the photocatalytic and antibacterial activity of Mn and S co-doped TiO_2 nanomaterial synthesized by the sol-gel method. Various instrumental techniques, XRD, BET, UV-Vis-DRS, TEM, XPS, SEM, FT-IR, were used to classify the catalyst samples. The characterization results show that the surface area is large, the particle size is small, band gap energy is low, the crystallite size is small, and the surface morphology is smooth. The efficiency of photocatalytic and antibacterial activity was evaluated by the degradation of Eosin yellow (EOY) and *Bacillus subtilis* (MTCC-441), respectively. The complete degradation of EOY was achieved in 70 min.

KEYWORDS TiO_2, Mn and S, sol-gel method, Eosin yellow, photocatalytic activity, antibacterial activity

FOR CITATION Kapuganti V. Divya Lakshmi, Tirukkovalluri Siva Rao, Gorli Divya Enhancement of photocatalytic and antibacterial activity performance of Mn–S co-doped TiO_2 nanocatalyst under visible light. *Nanosystems: Phys. Chem. Math.*, 2022, **13** (4), 438–444.

1. Introduction

Water is the largest part of vital substances for all existence on earth. It is known as a universal solvent, and it easily dissolves other substances. The aquatic environment can contain a wide range of micro pollutants, including pesticides, pharmaceuticals, and industrial compounds due to waste water effluent and agricultural runoff [1], mainly with reference to drinking water, which tends to become a limiting factor for the quality of life on earth. 25 % of pollution is caused by industries. They discharge hazardous materials to contaminate surface water and ground water. Toxic compounds enter into the water and reduce the quality [2, 3]. Dyes are used in many industries like paper, leather, textiles, plastic, ceramic, cosmetics, ink, food processing, etc. Wastewater offers eminent resistance to their biodegradation due to the presence of these heat and light-stable dyes, thus upsetting aquatic life [4]. While Eosin yellow (EOY) is commonly used for staining, it is regarded as a carcinogen. The current research strives to remove textile dyes and conduct an antibacterial study against *Bacillus subtilis* (MTCC-441), a gram-positive bacteria which causes pneumonia and septicaemia [5, 6]. The latest research focuses on the decontamination of polluted water and the elimination of dyes and pathogenic bacteria. TiO_2 is a semiconductor material widely used in photocatalytic reactions due to its non-toxicity, photo stability, and reusability [7–9]. The main drawback of TiO_2 is its wide bandgap energy (3.2 eV) and high recombination rate of photogenerated charge carriers, resulting in low quantum performance [10, 11]. As a result, changes to titanium have received a lot of attention, and several methods for increasing visible light photoactivity by doping with different metal and non-metal elements have been investigated [12, 13]. When compared to single-doped TiO_2, previous studies show that co-doped TiO_2 with metal and non-metal elements can enhance photocatalytic efficiency. Manganese is desired over all other transition metals because the t2g orbital of d is very close to the valence band, which causes the absorption to migrate to the visible region [14]. The photocatalytic activity of TiO_2 under visible light has been improved using a variety of non-metal materials, and the benefit of non-metal doping is that it reduces recombination centres. Sulfur is preferred since it replaces certain Ti^{4+} ions in the TiO_2 lattice [15, 16]. As a result, we chose Mn and S as dopants for the sol-gel method of synthesis of co-doped TiO_2. The main advantage of this method for preparing catalytic material is that it allows one to ensure excellent control of the product's properties through a variety of parameters such as ageing, homogeneity, grain size control, drying, and heat treatment [17].

2. Experiment

2.1. Materials

All of the chemicals used in the synthesis process were reagent grade, and the solutions were made with double distilled water. N-Butyl tetra ortho titanate ($Ti(OBu)_4$), Manganese nitrate $[Mn(NO_3)_2]\cdot 6H_2O$ and Thiourea were obtained from E-Merck (Germany) and used as Titanium, Manganese, and Sulfur precursors for the preparation of undoped TiO_2 and co-doped TiO_2 catalysts.

2.2. Preparation of Mn and S co-doped TiO_2 nano materials

The sol-gel method was used to make Manganese and Sulfur co-doped (1.0 Wt% Mn – 0.25 Wt% S) nano Titania. In this procedure, 20 mL of n-Butyl ortho titanate was added to ethanol and acidified with 3.2 mL of nitric acid in a beaker (solution-I) and stirred for 15 min. Manganese Nitrate and Thiourea were prepared by dissolving precursors of Mn and S in ethanol and adding deionized water (7.2 mL) to another beaker. A colloidal suspension formed after the complete addition of solution (II) was stirred for 90 min and aged for 48 h. The gel was dried at 70 °C in an oven, then ground and calcined in a muffle furnace at 450 °C for about 5 h. Finally, it was allowed to cool before being ground into a uniform powder. The same technique was used to make undoped TiO_2 but without the addition of sulfur and Manganese precursor.

2.3. Characterization of catalyst

Powder X-ray diffraction (XRD) spectra were taken (model: Ultima IV Rigaku) using anode Cu–WL 1 ($= 1.5406$ nm) radiation with a nickel filter to determine the crystalline structure of the photocatalyst. The applied current and voltage were 40 mA and 40 kV, respectively. The average crystallite size of anatase was determined according to the Scherrer equation using (FWHM) data of the selected peak. The size and shape of the nanoparticles were recorded with TEM measurements using JEOL/JEM 2100, operated at 200 kV. The morphology and elemental composition of the catalyst were characterized using scanning electron microscope (SEM) (ZEISS-SUPRA 55 VP) equipped with an energy dispersive X-ray (EDS) spectrophotometer and operated at 20 kV. The surface area and porosity measurements were carried out with a micrometrics Gemini VII surface area analyzer. The Nitrogen adsorption/desorption isotherms were recorded 2 – 3 times to obtain reproducible results and reported by BJH surface/volume mesopore analysis. The micropore volume was calculated using the Frenkel–Halsey–Hill isotherm equation. Each sample was degassed at 300 °C for 2 h. FT-IR spectra of the samples were recorded on FT-IR spectrometer (Nicolet Avatar 360). The diffuse reflectance spectra (DRS) were recorded with Shimadzu 3600 UV-Visible-NIR Spectrophotometer equipped with an integrating sphere diffuse reflectance accessory, using $BaSO_4$ as reference scatter. Powder samples were loaded into a quartz cell and spectra were recorded in the range of 200 – 900 nm. The extent of EOY degradation was monitored using UV-Vis spectrophotometer (Shimadzu 1601).

2.4. Photocatalytic activity

The photocatalytic performance of the synthesized catalyst Mn–S co-doped (MNS-5) nano titania was evaluated using the degradation of EOY dye under visible light irradiation in a photocatalytic reactor. A high-pressure 400 W (35,000 lm) mercury vapour lamp with UV filter was used as a visible light source (Oriel, 51472). The degradation procedure was carried out in a 150 mL Pyrex glass vessel with vigorous stirring positioned about 20 cm away from the light source, using 100 mL of EOY dye solution of necessary concentration (1 – 10 mgL^{-1}) containing adequate amount of the catalyst. The running water was circulated around the sample container to filter IR radiation to maintain constant solution temperature in a pyrex glass reaction vessel. The solution was stirred in dark for 30 min to attain adsorption-desorption equilibrium of EOY dye on the catalyst surface. After visible light illumination, small aliquots of sample were collected from the reaction mixture using Millipore syringe (0.45 μm) at different intervals of time to observe the change in EOY dye concentration by measuring the absorbance at 516 nm using UV-Visible (Milton Roy Spectronic 1201) Spectrophotometer. For investigation of pH variation during the degradation process, Elico Digital pH metre model 111E, EI was used. Prior to irradiation, the dye solutions' pH was adgusted with 0.1 N NaOH / 0.1 N HCl to achieve the desired pH. The following equation was used to determine the percent of EOY dye degradation (α):

$$\alpha = \frac{A_0 - A_t}{A_0} \cdot 100\ \%,$$

where A_0 represents the initial absorbance of the dye solution prior to degradation and A_t represents the absorbance of the dye solution at time t.

The optimum reaction conditions are attained by varying the reaction parameters, such as dopant concentration, effect of pH, catalyst dosage, and initial dye concentration, and the results are discussed in Sections 4.1 – 4.4.

2.5. Antibacterial activity study

The Agar-well diffusion method was used to study the antibacterial activity of MNS-5 against the Gram-positive bacteria *Bacillus subtilis* (MTCC-441). In a 100 mL conical flask, nutrient agar (High media – India) was dissolved in water and sterilised in an autoclave at 121 °C 15 lbp for 15 min. The media was autoclaved before being poured onto sterilised petri dishes. A sterile cork-borer was used to make the wells. Different concentrations of TiO_2 co-doped (MNS-5) nanoparticles are injected into wells in petri plates (200, 300 and 400 μg/mL). The TiO_2 nanoparticles were dispersed in sterile water and used as a negative control, while the normal antibiotic Chloramphenicol (100 μg/mL) was used as a positive control.

3. Characterizations

The synthesized catalysts was characterized by X-ray diffraction (XRD), X-ray photo electron spectroscopy (XPS), Scanning electron microscopy (SEM), Energy dispersive X-ray Spectroscopy (EDX), Fourier transform infrared spectroscopy (FT-IR), UV-Visible Diffused Reflectance Spectroscopy (UV-Vis-DRS), Transmission electron Microscopy (TEM) and Brunauer–Emmett–Teller (BET). In XRD, all the diffraction peaks represented the anatase phase with a characteristic high intensity peak at $2\theta = 25.50$ and small peaks corresponding to 2θ values at 37.9, 48.4, 54.8, and 62.6 °, which can be indexed as (101), (004), (200), (105), (211) and (204) planes of anatase TiO_2 (JCPDS card no. 21-1272) respectively. The SEM results in agglomeration and particle size can be inferred from this because of the co-doping of Mn and S into TiO_2. The Mn and S contents in MnS-5 are greatly reduced. Their presence was confirmed by EDX analysis. The FT-IR study confirms that Mn and S are substitutionally doped in the TiO_2 lattice by replacing Ti^{4+} ions. The TEM images illustrated that the undoped and co-doped TiO_2 (MnS-5) nanocatalysts are small in size with a spherical shape. The diffused reflectance spectra (DRS) of undoped and co-doped TiO_2 samples are observed to show remarkable decreases in band gap and extension of the absorption edge towards longer wave lengths. The X-ray photo electron spectroscopy (XPS) analysis of MnS-5 revealed the dopant elements such as (Mn, S). This indicates that the dopant elements are incorporated into the TiO_2 lattice. The co-doped samples of MnS-5 have high surface areas of 155.878 m^2/g, pore volumes of 0.204 cm^3/g, and pore diameters of 4.8 nm. This could be because a catalyst with larger surface area stimulates the adsorption of more dye molecules.

The characterization results are reported in the previous article [18].

4. Evaluation of photocatalytic efficiency of catalyst (MNS-5) by degradation of Eosin yellow (EOY)

The effect of reaction parameters such as dopant concentration, pH, catalyst dose, and initial dye concentrations on the photocatalytic degradation of EOY was investigated by varying the desired parameter while keeping the other parameters constant.

4.1. Effect of dopant concentration

Figure 1 illustrates the photocatalytic degradation of the EOY dye (516 nm) by a synthesized catalyst. The co-doped samples showed increased photocatalytic activity compared to undoped TiO_2 under visible light irradiation. The possible reason is that the dopant concentration contributes to a reduced TiO_2 band gap, smaller particle size, and a larger surface area of the catalyst among the different co-doped catalysts. At this dopant concentration, photo generated electron/hole pairs can easily pass to the catalyst surface through Mn, resulting in oxidative species such as $OH\cdot$, $O_2\cdot$, and $HO_2\cdot$.

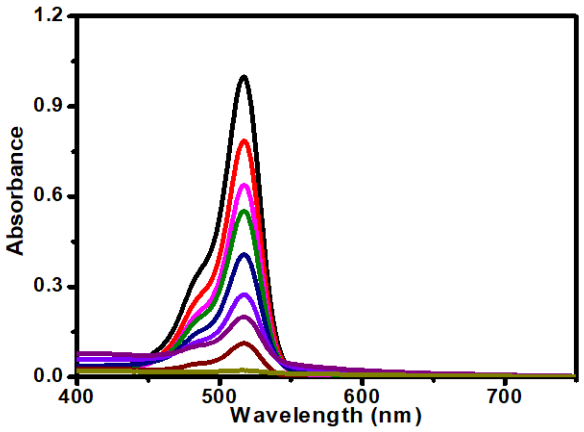

FIG. 1. Effect of dopant concentration on photocatalytic of co-doped Titania for rate of degradation of EOY dye. Here, catalyst dosage 100 mg/L, pH 4 and EOY = 10 mg/L

4.2. Effect of pH

The electrostatic interactions between the catalyst surface dye and charged radicals are dependent on the pH of the solution, pH is a significant variable parameter in the evaluation of photocatalytic dye degradation efficiency of the catalyst in aqueous medium [19]. Fig. 2 depicted the percentage degradation of EOY using the MNS-5 catalyst at various pH values (2, 4, 8 and 10) when exposed to visible light. The percentage of EOY degradation in acidic medium is higher than in basic medium, as shown in the figure. This may be due to a stronger electrostatic interaction between the catalyst's positively charged surface and the negatively charged dye molecules. As the pH is raised to a basic medium, the catalyst surface takes on a -Ve charge and repels the same charged dye molecules electrostatically. In acidic pH medium, the percentage of degradation of EOY was high at pH 4, at which the positive charge (H^+ ions) on TiO_2 surface increases and negatively charged EOY can easily adsorbed on the catalyst surface.

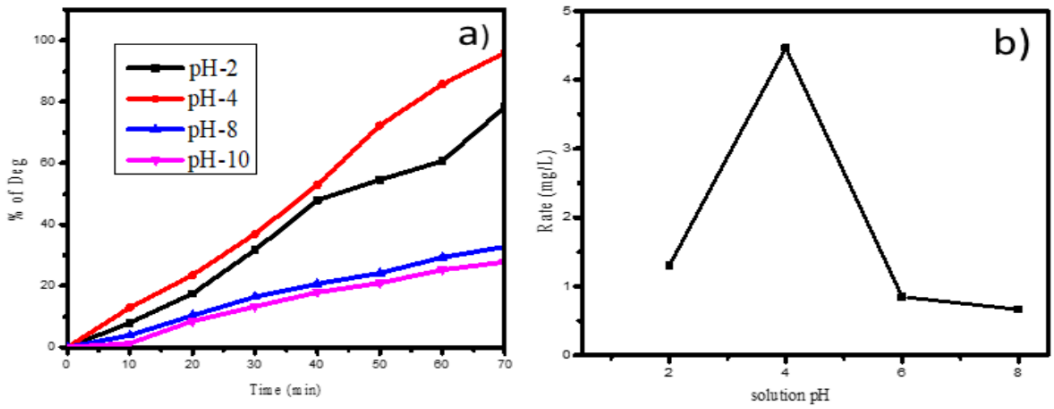

FIG. 2. The effect of pH on the rate of degradation of EOY dye by Mn 2p & S 2p co-doped TiO_2. Here, catalyst dosage 100 mg/L and EOY =10 mg/L

4.3. Effect of catalyst dosage

The effect of catalyst dosage on the degradation of EOY is shown in Fig. 3. The rate of degradation was carried out by varying the catalyst amounts of 0.05, 0.10, 0.15, and 0.20 g added to 100 mL of solution containing 10 mg/L of dye at pH 4. The rate of degradation increases linearly with the increase of catalyst loading up to 0.10 g. Degradation decreases as the catalyst dosage is increased. This may be due to increased turbidity and agglomeration of catalyst particles, which prevent light from penetrating to activate the catalyst particles [20], as well as collisions between active molecules and ground state molecules of co-doped TiO_2 result in catalyst particle deactivation [21]. Hence, the optimum catalyst dosage is 0.10 g.

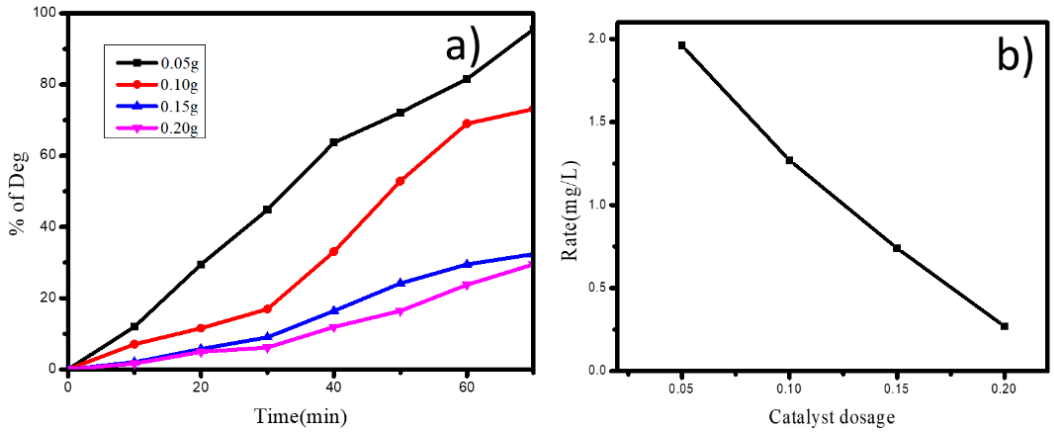

FIG. 3. Effect of catalyst dosage on the degradation of EOY by MNS-5 co-doped TiO_2 here pH = 4 and EOY =10 mg/L

4.4. Effect of initial concentration of dye (EOY)

Experiments were carried out with different concentrations of EOY dye from 5 to 30 mg/L to research the effect of initial dye concentration (EOY) at fixed weight of catalyst dose (10 mg/L) and pH 4, and the graphs were plotted in Fig. 4. These results show that the rate of EOY dye degradation increased by up to 10 mg/L. However, due to the blanket effect, raising the dye concentration causes the catalyst to deactivate, slowing the rate of degradation [22].

5. Antibacterial studies

The antibacterial activity of TiO_2 nano particles was investigated using the Agar-well diffusion method [23] against *Bacillus subtilis* (MTCC-441) and varying concentrations of co-doped TiO_2 (MNS-5) nanoparticles which were placed in different wells in a petri dish with concentrations ranging from 200, 300, 400 μg/mL, and chloromphenicol (control). The activity results (Fig. 5 and Table 1) showed that (400 μg/ml) is the best concentration for co-doped TiO_2 for the zone of inhibition of both bacteria and is also very nearer to the standard values. As a result, the co-doped TiO_2 nanoparticles have higher antibacterial activity. This inhibition could be caused by an e–/h+ that occurs in the valence band of TiO_2 when the catalyst is exposed to visible light. This e–/h+, +ve hole acts as a strong oxidising agent under visible light, destroying the bacterial protein coat and inhibiting the growth of the organism.

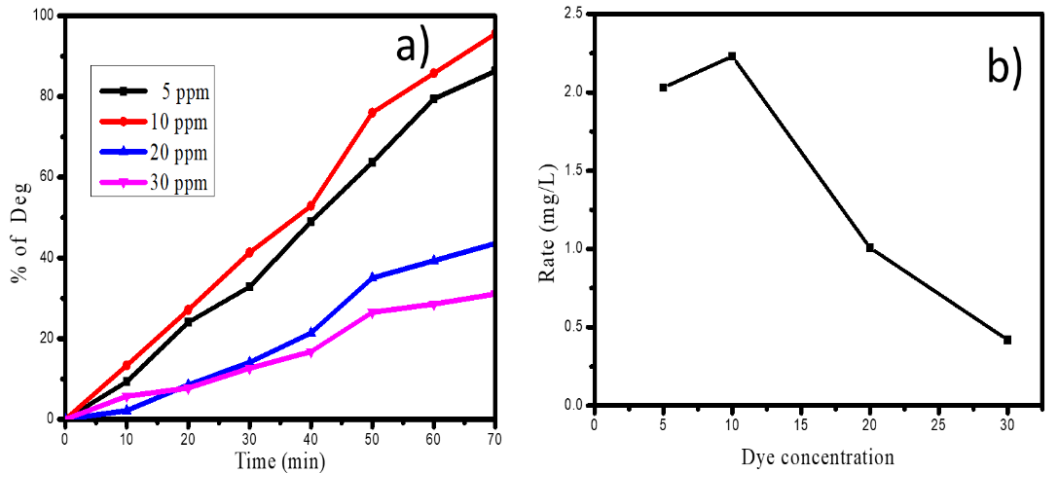

FIG. 4. Effect of initial concentration of the dye on the rate of degradation of EOY dye Here, pH = 4 and catalyst dosage – 100 mg/L

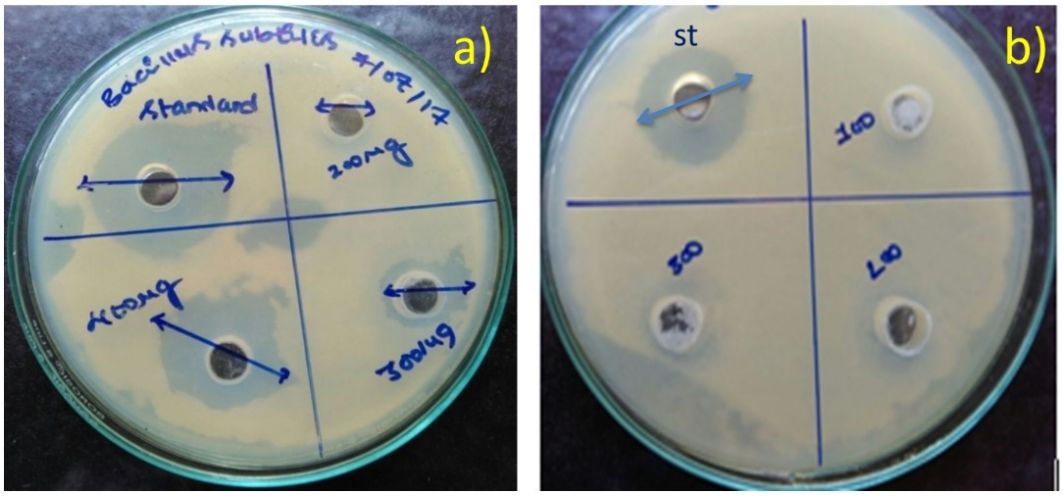

FIG. 5. Zone of inhibition of *Bacillus subtilis* (MTCC-441) (a); undoped TiO_2 (b)

TABLE 1. Agar-well diffusion of co-doped TiO_2 nanoparticles (MNS-5) *Bacillus subtilis* (MTCC-441) and undoped TiO_2

s. no	Catalyst	Organism	Zone of inhibition (mm)			
			200 μg/mL	300 μg/mL	400 μg/mL	Standard (Chloramphenicol) 100 μg/mL
1	MNS-5	*Bacillus subtilis* (MTCC-441)	9	11	**24**	25
2	Undoped TiO_2	*Bacillus subtilis* (MTCC-441)	—	—	—	24

6. Conclusion

The Mn and S co-doped anatase TiO_2 was effectively synthesized using the sol-gel method, and it was later characterized using different analytical methods. In Mn and S co-doped TiO_2, Sulfur causes the shift in the absorbance band of TiO_2 from the UV to visible region, whereas doping of Mn inhibits the electron/hole recombination and acts as a charge carrier during photocatalytic degradation under visible light irradiation. As compared to undoped TiO_2, co-doped TiO_2 with 1.00 wt % Mn and 0.25 wt % S had a small particle size and a high surface area. The resulting Eosin yellow (10 ppm) was successfully degraded by 0.10 g co-doped catalyst (MNS-5) at pH 4 in 70 min, as well as MNS-5 demonstrating good antibacterial activity against *Bacillus subtilis* (MTCC-441). It is possible to infer that Mn and S co-doped TiO_2 has increased photocatalytic activity and is an efficient antibacterial agent.

References

[1] Pirbazaria A.E., Monazzama P., Kisomi B.F. Co/TiO_2 Nanoparticles: preparation, characterization and its application for photocatalytic degradation of methylene blue. *Desalination and Water Treatment*, 2017, **63**, P. 283–292.

[2] Zhang H., Tang Q., et al. Enhanced photocatalytic properties of PET filament coated with Ag–N co-doped TiO_2 nanoparticles sensitized with Disperse blue dyes. *Nanomaterials*, 2020, **10**, 987.

[3] Basavarajappa P.S., Patil S.B., et al. Recent progress in metal-doped TiO_2, non-metal doped/co-doped TiO_2 and TiO_2 nanostructure hybrids for enhanced photocatalysis. *Int. J. of Hydration Energy*, 2020, **45**, P. 7764-7778.

[4] Manga Raju I., Siva Rao T., et al. Poly 3-Thenoic acid sensitized, Copper doped anatase/brookite TiO_2 nanohybrids for enhanced photocatalytic degradation of an organo phosphorus pesticide. *J. of Env. Chem. Eng.*, 2020, **7**, 103211.

[5] Anirudhan T.S., Rejeena S.R. Photocatalytic Degradation of Eosin yellow using poly (pyrrole-co-aniline)-coated TiO_2/nanocellulose composite under solar light irradiation. *J. of Materials*, 2015, 636409.

[6] Yuan Y., Ding J., et al. TiO_2 Nanoparticles co-doped with Silver and Nitrogen for antibacterial application. *J. of Nanoscience and Nanotech.*, 2010, **10**, P. 4868–4874.

[7] Alim S.A., Siva Rao T., et al. Fabrication of visible light driven nano structured Copper, Boron co-doped TiO_2 for photocatalytic removal of Lissamine Green B. *J. of Saudi Chem. Soc.*, 2018, **23**, P. 92–103.

[8] Vasilevskaia A.K., Popkov V.I., Valeeva A.A., Rempel A.A. Formation of Nonstoichiometric Titanium Oxides Nanoparticles Ti_nO_{2n-1} upon heat-treatments of Titanium hydroxide and anatase nanoparticles in a hydrogen flow. *Russ. J. of Appl. Chem.*, 2016, **89**, P. 961–970.

[9] Popkov V.I., Bachina A., et al. Synthesis, morphology and electrochemical properties of spherulite titania nanocrystals. *Ceramics Int.*, 2020, **46** (15), P. 24483–24487.

[10] Lee S.Y., Dooho K., et al. Photocatalytic degradation of Rhodamine B dye by TiO_2 and gold nanoparticles supported on a floating porous Polydimethylsiloxane sponge under ultraviolet and visible light irradiation. *ACS Omega*, 2020, **8**, P. 4233–4241.

[11] Audina Putri R., Safni S., et al. Degradation and mineralization of violet-3B dye using C–N co-doped TiO_2 photocatalyst. *Env. Eng. Research*, 2020, **25**, P. 529–535.

[12] Mancuso A., Sacco O., et al. Enhanced visible-light-driven photo degradation of Acid Orange 7 azo dye in aqueous solution using Fe–N co-doped TiO_2. *Arabian J. of Chem.*, 2020, **13**, P. 8347–8360.

[13] Sharotri N., Sharma D., Sud D. Experimental and theoretical investigations of Mn-N-Co-doped TiO_2 photocatalyst for visible light induced degradation of organic pollutants. *J. of Materials Research and Technology*, 2019, **8**, P. 3995–4009.

[14] Abderrahim E., Logvina M.V., et al. Synthesis of Fe- and Co-doped TiO_2 with improved photocatalytic activity under visible irradiation toward Carbamazepine degradation. *Materials*, 2019, **12**, 3874.

[15] Bayan E.M., Lupeiko T.M., et al. Zn–F co-doped TiO_2 nanomaterials: Synthesis, structure and photocatalytic activity. *J. of Alloys and Compounds*, 2020, **82**, 153662.

[16] Divya Lakshmi K.V., Siva Rao T., et al. Structure, photocatalytic and antibacterial activity study of meso porous Ni and S co-doped TiO_2 nanomaterial under visible light irradiation. *Chinese J. of Chem. Eng.*, 2019, **27**, P. 1630–1641.

[17] Singla P., Pandey O.P., Singh K. Study of photocatalytic degradation of environmentally harmful phthalate ester using Ni-doped TiO_2 nanoparticles. *Int. J. of Environmental Science and Technology*, 2016, **13**, P. 849–856.

[18] Divya Lakshmi K.V., Siva Rao T., et al. Visible light driven mesoporous Mn and S co-doped TiO_2 nano material: characterization and applications in photocatalytic degradation of Indigocarmine dye and antibacterial activity. *Enviromental Nanotechnology, Monitoring & Management*, 2018, **10**, P. 494–504.

[19] Manamon C., John O.C., et al. A facile route to synthesis of S-doped TiO_2 nanoparticles for photocatalytic activity. *J. of Molecular Catalalysis A: Chemical*, 2015, **406**, P. 51–57.

[20] Thanh Le T.T., Trinh Dinh T. Photocatalytic degradation of Rhodamine B by C and N codoped TiO_2 nanoparticles under visible-light irradiation. *J. of Chemistry*, 2020, 4310513.

[21] Alok Garg, Tejasvi Singhania, et al. Photocatalytic degradation of Bisphenol-A using N, Co co-doped TiO_2 catalyst under solar light. *Sci. Report*, 2019, **9**, 765.

[22] Mahlambi M.M., Mishra A.K., et al. Comparison of Rhodamine B degradation under UV irradiation by two phases of titania nano-photocatalyst. *J. of Thermal Analysis and Colorimetry*, 2012, **110**, P. 847–855.

[23] Ahmad T., Phul R., Khatoon N., Sardar M. Antibacterial efficacy of Ocimum Sanctum leaf extract-treated Iron oxide nanoparticles. *New J. Chem.*, 2017, **41** P. 2055–2061.

Submitted 5 January 2022; revised 9 July 2022; accepted 1 August 2022

Information about the authors:

Kapuganti V Divya Lakshmi – Sri Satya Sai University for Human Excellence, Kalaburagi, Karnataka, India; Department of Inorganic and Analytical Chemistry, Andhra University, Visakhapatnam 530003, India; kdivyalaxmi@gmail.com

Tirukkovalluri Siva Rao – Department of Inorganic and Analytical Chemistry, Andhra University, Visakhapatnam 530003, India; ORCID-0000-0002-6558-5762; Telephone: +91891-2844667; Mobile: +91 7702110459; sivaraotvalluri.16@gmail.com

Gorli Divya – Department of Inorganic and Analytical Chemistry, Andhra University, Visakhapatnam 530003, India; gorlidivya@gmail.com

Conflict of interest: the authors declare no conflict of interest.